OPTIMAL PLACEMENT OF EXCITATIONS AND SENSORS BY SIMULATED ANNEALING

M. Salama, R. Bruno, G-S. Chen, and J. Garba
Applied Technologies Section
Jet Propulsion Laboratory
California Institute of Technology

BACKGROUND

It is often desired in many applications to optimally select the locations of a given number of discrete actuators and response measurements. For example, ground modal testing involves the determination of the structural dynamic characteristics (frequencies, modes, and damping) from forced vibration tests. The locations of excitations and measurements are usually assigned on the basis of skilled engineering insight. After intensive processing and review of the test data, it may be further required to perform additional testing for a different set of excitation and measurement locations. The process is repeated until satisfactory results have been obtained for all modes of interest.

Repeated experimentation and data review is a luxury that cannot be afforded in the on-orbit verification of the dynamics of complex large structures which have been assembled or deployed for the first in space in their service configuration. Especially in the latter case, it is essential to determine in advance the number and locations of required excitations such that the quality and quantity of information derived from a single set of measurements are maximized.

When the locations available for placement of the excitation and measurement devices are spatially continuous, the usual gradient - based optimization methods can be used successfully to determine the optimum locations. However, when the available locations are spatially discrete, the problem becomes one of integer or combinatorial optimization. Except for the simplest cases, combinatorial optimization problems tend to be nonconvex and to require the evaluation of very large numbers of combinations of possible locations - thus becoming computationally intractable. Their exact solution is usually not possible with reasonable expenditure of computing resources. Thus instead of seeking the exact optimum, one must resort to suboptimal approximate techniques, most of which are heuristically-based [1, 2, 3]. In this paper, we further pursue the method of simulated annealing of Ref. [3] with the objective of (1) exploring a number of improvements which aim at incorporating knowledge about the structural characteristics in the random search of the simulated annealing method, and (2) applying the technique to the problem of finding the optimal location of passive dampers.

OPTIMIZATION STATEMENT

The optimal placement problem at hand may be stated as follows:

Given I* sensors that may be placed at any of I possible discrete locations, and given J* actuators that may be placed at any of J possible discrete locations, find the combination of location C(I*, J*), I*ϵI, J*ϵJ which extremize an objective function E(I*,J*), Figure 1.

The specific choice of the objective function E, and whether it should be maximized or minimized is problem dependent. It may be taken to represent a structural property or a response quantity. And just as in the continuous optimization problems, side constraints may be imposed on the design variables (locations of I* and J*) or any function thereof h(I*, J*). In some cases, the design variables may consist of sensor locations only or actuator locations only. When both are present, their co-location may be admitted.

$$\text{Find } C(I*, J*); \quad I*\epsilon I; \quad J*\epsilon J \tag{1}$$

$$\text{Such that } E(I*, J*) \rightarrow \text{EXTREMUM} \tag{2}$$

$$\text{Side constr. } \overline{h} \geq h(I*, J*) \geq \underline{h} \tag{3}$$
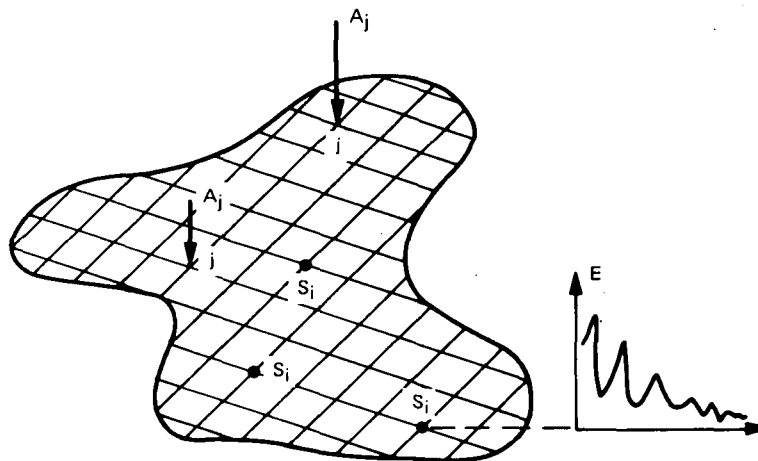

Figure 1.

COMPUTATIONAL COMPLEXITY

Through enumeration, it is possible to determine the exact solution to the problem stated previously by evaluating the objective function for every possible combination of I* sensor locations and J* actuator locations. This is a combinatorial optimization problem for which the number of possible combinations that must be examined can be found from

$$\eta^* = \frac{I!}{I^*!(I-I^*)!} \times \tfrac{1}{2} \left[\frac{J!}{J^*!(J-J^*)!} +1\right] \tag{4}$$

The ($\tfrac{1}{2}$) and (+1) account for Maxwell's reciprocity theorem relating locations of actions and response. Table 1 below gives numerical values for η^* for various parameter values. Clearly, the number of possible combinations that must be evaluated becomes extremely large rather rapidly for problems with relatively small order.

Table 1

I	I*	J	J*	η^*
5	3	5	2	55
20	5	20	2	1.48×10^6
100	10	50	5	1.84×10^{19}
1000	100	500	10	$\sim \infty$

Intractable, Except for Simplest Cases

ITERATIVE IMPROVEMENT TECHNIQUES

Most conventional techniques for finding approximate solutions to combinatorial optimization problems are built around the idea of iterative improvements. Starting with an initial solution, iterative improvement techniques repeatedly consider changes in the current solution and accept only those that improve the objective function, see Figure 2. The disadvantage of these techniques is that they usually get trapped in a local optimum. Without a mechanism to allow climbing out of local optima, they will fail to discover more global ones. The simulated annealing technique provides such a mechanism and may be considered a variation on iterative improvement algorithms.
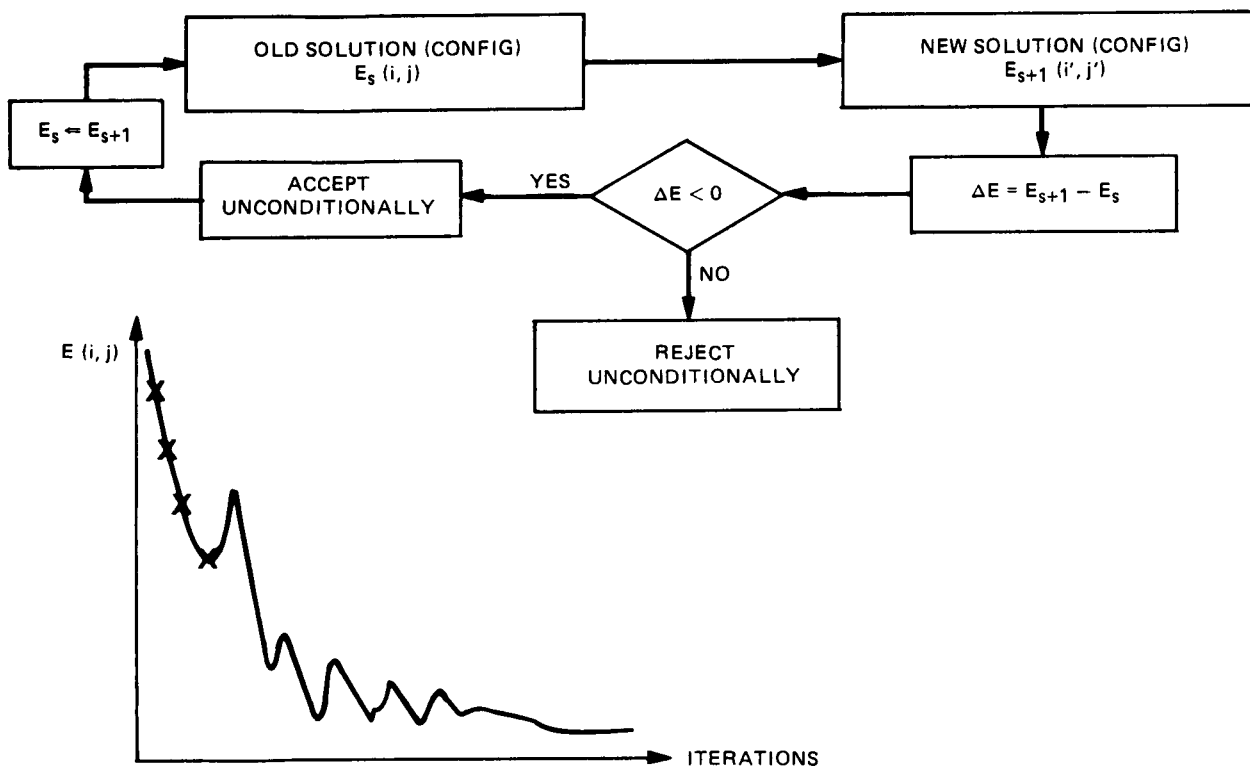

Figure 2.

THE SIMULATED ANNEALING HEURISTIC

In trying to numerically simulate the behavior of atoms of a body in thermal equilibrium at finite temperature, Metropolis et al. [4] observed that at high temperature T_h the atoms are randomly arranged in a state of disorder whose energy level is high. Following Figure 3, as the temperature T_h is cooled to T_0, the atoms migrate to a more ordered state having low energy level. The final degree of order depends on the cooling rate. Too fast cooling (quenching) is characterized by a monotonic decrease in energy to an intermediate state of semi-order. On the other hand slow cooling (annealing) is characterized by a general decrease in energy accompanied by occasional small energy increases whose rate of occurrence may be estimated by the probability density

$$P = 1/(e^{\Delta E/K_B T}) \tag{5}$$

where ΔE is the change in energy, K_B is a Boltzmann constant, and T is the current temperature. At the low temperature end of the annealing process the system's energy reaches a much lower value (ground state) and the atomic arrangement reaches a much higher degree of order (Crystaline) than in the rapid quenching regime. Annealing, therefore, allows achieving a more global energy optimum than is possible by the local optimum provided by rapid quenching.

Use of the annealing simulation algorithm as an optimization tool is, therefore, built on the premise that in anticipation of reaching a more globally optimum solution, we must occasionally accept deteriorating ones. The probability of accepting deteriorating solutions is given by Equation (5). And it is these probabilistic jumps that allow the solution to climb out of local optima.
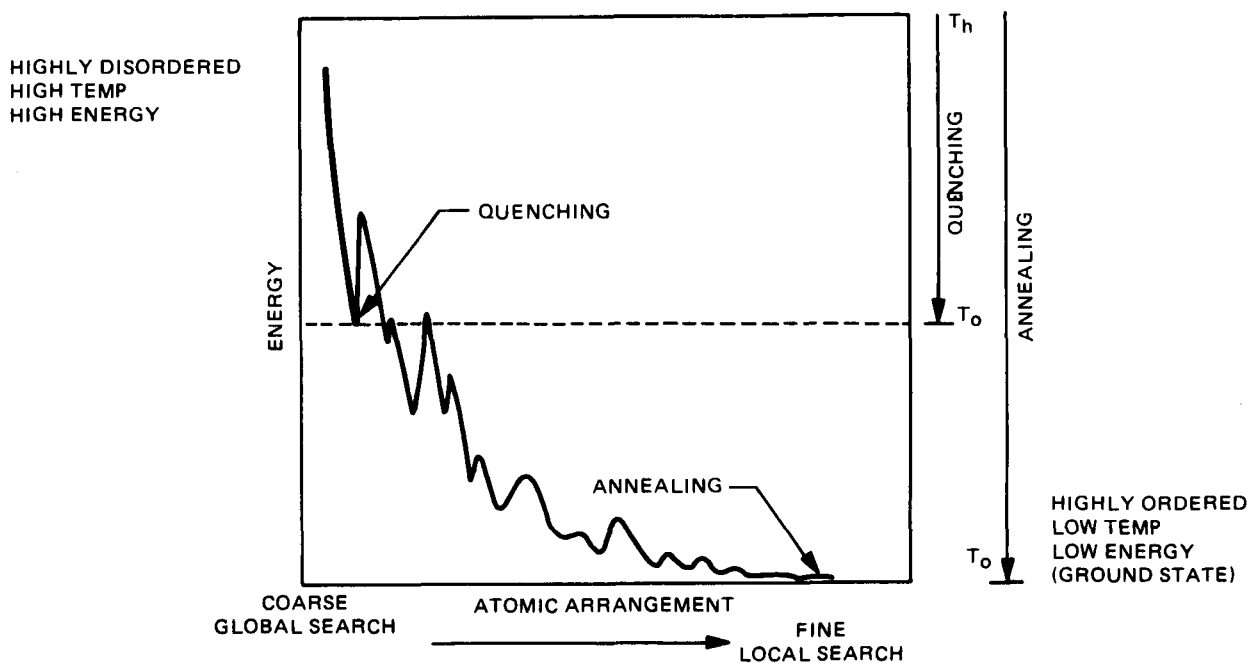
Figure 3.

SIMULATED ANNEALING ALGORITHM

The flow chart in Figure 4 outlines steps of the simulated annealing heuristic just described. It differs from the iterative improvements algorithm mainly in the introduction of the probability function which controls the frequency of accepting deteriorating solutions. As an optimization tool, the simulated annealing method does not involve any actual annealing or temperature. The product K_BT is replaced by θ which may be viewed as a pseudo temperature, a parameter that controls the frequency of accepting deteriorating solution during the optimization process. Notice that the probability density function P, ranging from 1.0 to zero, is highest at high pseudo temperature θ_h, (i.e., at the beginning of the optimization iterations). The algorithm therefore begins with a coarse global search where more deteriorating solutions are accepted (P $-$ 50% to 80%), and gradually ends up with fine local search where only improving solutions are accepted. As the optimization procedure continues iteratively, new solutions or configurations must be generated. For the type of problems under consideration, a new solution or configuration is defined by a set of locations for I* sensors and J* excitations. In an earlier application of the method [3], new solutions were generated from the current one by moving the J* excitations one at a time randomly to any of the remaining (J-J*) unassigned locations, and moving the I* sensors one at a time randomly to any of the remaining (I-I*) unassigned locations. Variations on this scheme will be explored subsequently.
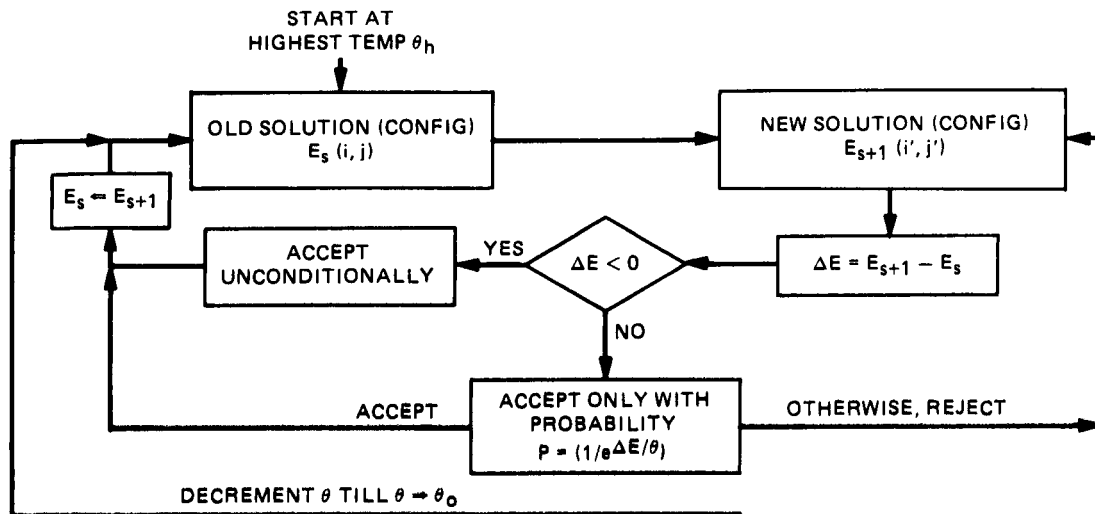
START AT
HIGHEST TEMP θ_h

OLD SOLUTION (CONFIG)
E_s (i, j)

NEW SOLUTION (CONFIG)
E_{s+1} (i', j')

$E_s \leftarrow E_{s+1}$

$\Delta E = E_{s+1} - E_s$

$\Delta E < 0$

YES

ACCEPT UNCONDITIONALLY

NO

ACCEPT

ACCEPT ONLY WITH PROBABILITY
$P = (1/e^{\Delta E/\theta})$

OTHERWISE, REJECT

DECREMENT θ TILL $\theta \rightarrow \theta_0$

Figure 4.

OPTIMAL LOCATIONS OF PASSIVE DAMPERS

1. DESCRIPTION

The cantilevered truss shown in Figure 5 consists of 58 axial
members connecting 23 pinned joints with 114 unrestrained degrees
of freedom. The modal masses are not uniformly distributed; 55%
of the mass is concentrated near the free tip. The first nine
undamped frequencies and a qualitative description of their
corresponding modes are listed in Table 2. While the first few
modes are primarily global in nature, higher modes of the truss
are primarily local with much of the strain energy tending to be
concentrated at members near the free tip. Assuming no inherent
structural damping, we wish to place a limited number of passive
dampers N_D along some members of the truss so as to achieve a
desired level of modal damping ζ_i in any specified mode i. If we
further assume that the target modal damping ζ_i per cycle is to be
adjusted so that the total decay over one second of time is
constant = 17.4% for any mode, then $\zeta_i = .174/\Omega_i$. These are also
listed in Table 2.

Table 2

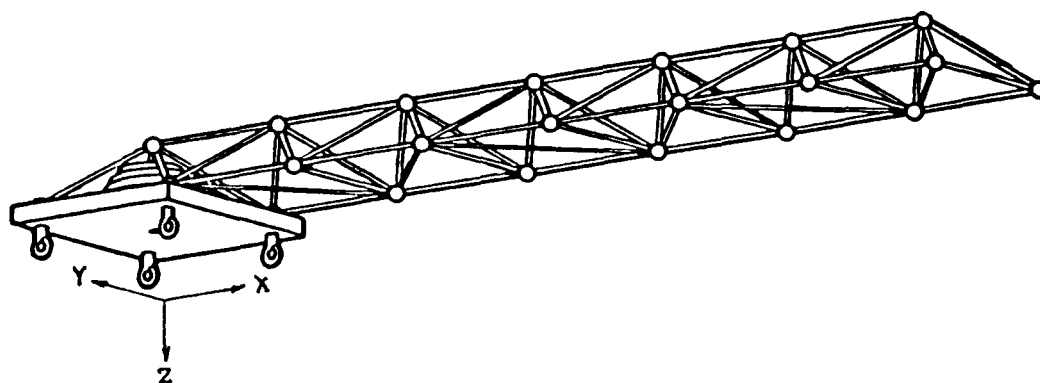| Mode No.	1	2	3	4	5	6	7	8	9
Freq. (Hz)	8.7	15.5	33.0	60.0	71.3	74.2	79.5	88.2	95.1
Mode Type	1st xz	1st xy	1st torsion	Comb. xy xz	2nd xz	local bending & twisting almost near tip			
Target Modal Damping ζ_i	2%	1.12%	.53%	.29%	.24%	.23%	.22%	.20%	.18%

Figure 5.

OPTIMAL LOCATION OF PASSIVE DAMPERS

2. PERFORMANCE INDEX

With the quantities defined below, one may define the performance index J_e as a measure of performance over all N_m modes under consideration. Maximization of J_e over all possible combinations of N_D damper locations will insure the highest possible modal damping ζ_i for modes $i=1,\ldots,N_m$.

The specific form of the performance index J_e below is motivated by the fact that for $r=2$, $N_m=2$, a geometrical interpretation can be given: if e_1 and e_2 represented two perpendicular sides of a triangle, the maximum value for J_e for a constant $(e_1 + e_2)$ will occur when $e_1 = e_2$. This interpretation may be generalized to any hyper-dimension N_m and for any $r>2$. More importantly, this means that maximization of J_e will insure the maximization of all e_i quantities more equally. The higher the r-values, the more sensitive will J_e be to small changes in e_i. In the following numerical results, $r=4$ was used.

DEFINE: $\zeta_o = 5\% =$ percent damping provided by any of N_D passive damping elements

$\epsilon_{ij} =$ strain energy ratio imparted in mode i to truss member j

$\zeta_i =$ percent modal damping computed for mode i

$$= \sum_{j=1}^{N_D} \zeta_o \, \epsilon_{ij}$$

$e_i = \zeta_i/\bar{\zeta_i} =$ normalized modal damping for mode i

OBJECTIVE: maximize the performance index J_e

$$J_e = \left(\frac{1}{N_m} \sum_{i=1}^{N_m} (e_i)^{1/r}\right)^r \qquad r \geq 2 \qquad (6)$$

3. NUMERICAL RESULTS

In what follows, two cases are considered. They differ in the number of passive elements N_D used, and the number of modes N_m targeted for modal damping alteration. In case 1, four passive damping elements are used to achieve the target modal damping in the first three modes. In case 2, six passive damping elements are used to achieve the target modal damping in all nine modes. The optimal locations found by the simulated annealing technique are indicated in Figure 6 by 1 and 2, for case 1 and case 2, respectively. The corresponding modal damping values are given by mode for each case in Table 3. Note that all target values have been exceeded for both cases, except for mode 3 in the second case. This could also be satisfied with the addition of a seventh damper.

Table 3

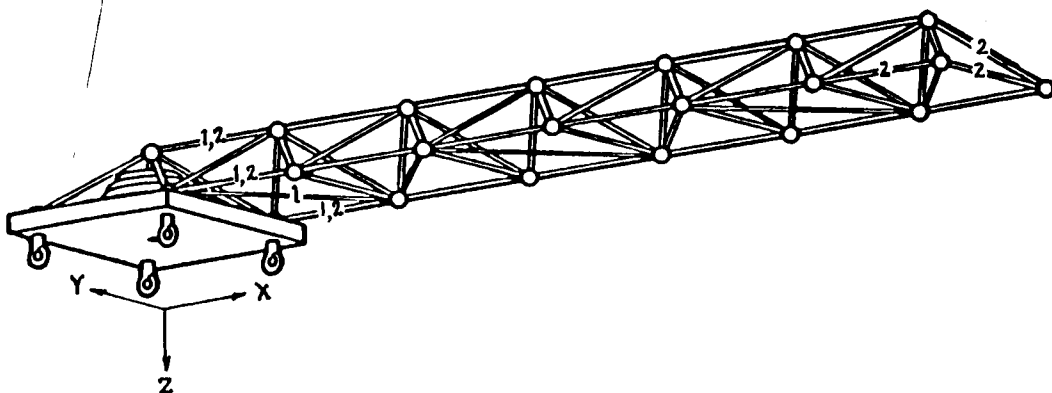|	Mode No.	1	2	3	4	5	6	7	8	9
Case 1 $N_D=4$ $N_m=3$	Target ζ_i	.02	.0112	.0053	.0029	.0024	.0023	.0022	.0020	.0018
	Computed ζ_i i=1,..3	.0207	.0203	.0065						
Case 2 $N_D=6$ $N_m=9$	Computed ζ_i i=1,..,9	.0208	.0193	.0038	.0330	.0160	.0341	.0304	.0393	.0201

Figure 6.

ITERATION HISTORY FOR FOUR PASSIVE DAMPING ELEMENTS

An insight into how the algorithm converges can be gained by examination of the iteration history in Figure 7 for four passive damping elements. Convergence was achieved after about 200 solutions steps. As a result of the probability function used, the solutions began with large variations (in both amplitude and frequency) about a trend line (dotted). Gradually, these variations are damped out. Note that an enumeration (exact) solution to this problem would require $58!/[4!(58-4)!] = 424,270$ evaluations.
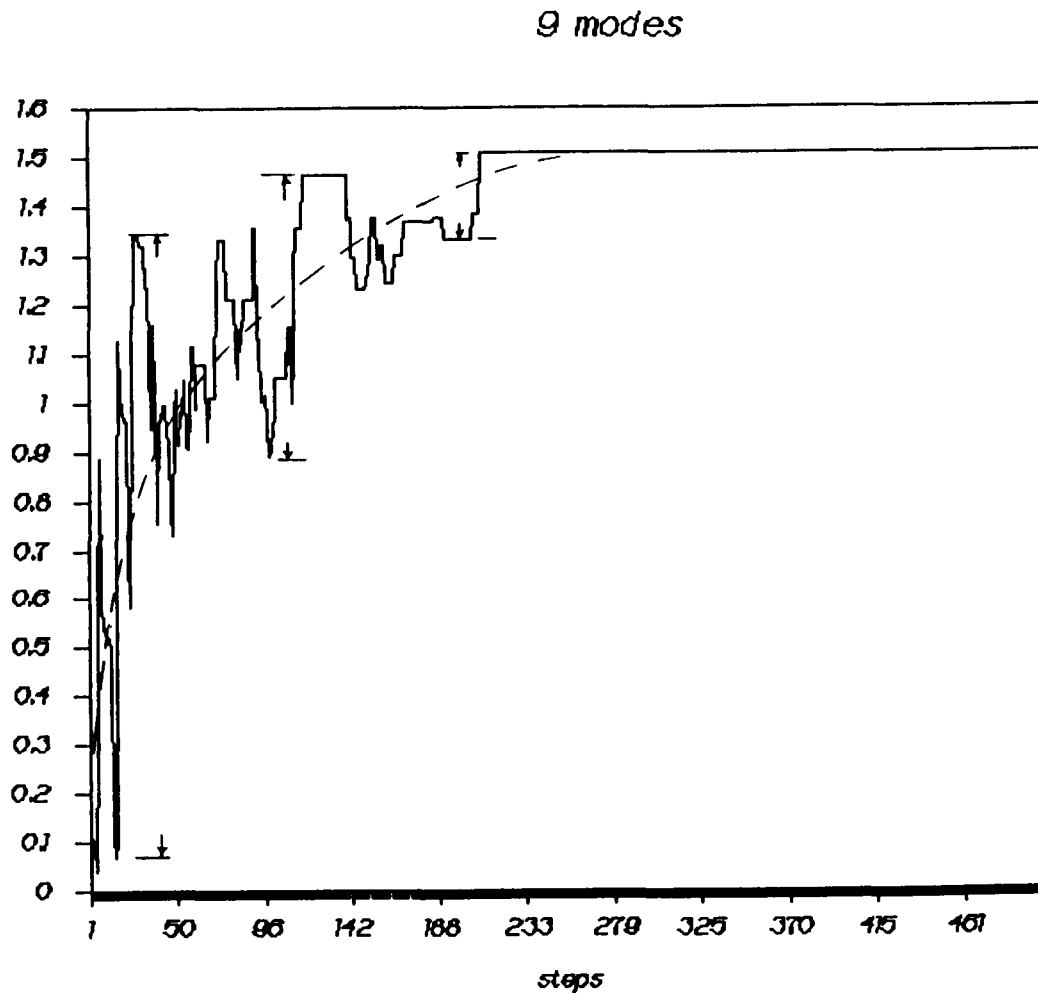
9 modes

Figure 7.

OPTIMAL PLACEMENT OF EXCITATIONS & SENSORS

In this section, we revisit the previously solved example of the COFS space truss [3], with the aim of introducing a number of improvements in the policy of generating new solutions during the simulated annealing optimization. The objective here is to place I* sensors and J* actuators so as to maximally observe all first thirteen modes of the 960 degrees of freedom truss structure. In general, all N=960 degrees of freedom are possible sites for excitation and sensing. In practice, however, only a subset I are allowed for sensing using I* sensors (I*ϵ I ϵ N), and only a subset J are allowed for excitation using J* actuators (J* ϵ J ϵ N). Co-location of sensors and actuators is admitted, and only one sensor and one actuator may be placed at a degree of freedom.

Taking the kinetic energy $E_i{}^j$ measured at degree of freedom i due to excitation at degree of freedom j to be the observer for the selected N*=13 modes, one can form the objective function to be maximized as given below. Instead of the kinetic energy $E_i{}^j$, one may choose to observe the square of the displacement $U_i{}^j$. The general form of the objective function remains the same, but the optimal locations are expected to be different. This is illustrated by the numerical results in Figure 8 for the three cases listed in Table 4 below.

OBJECTIVE: Place a Given Number of Sensors and Excitations
so as to Maximally Observe a Given Number of Modes.

$$\underset{I^*,J^*}{\text{Max}} \left[\sum_n^{N^*} \sum_m^{N^*} \left(\sum_{j=1}^{J^*} \sum_{i=1}^{I^*} E_i{}^j \right)^{1/r} \right]^r , \quad (I^* \,\epsilon\, I \,\epsilon\, N), \quad (J^* \,\epsilon\, J \,\epsilon\, N)$$

$$E_i{}^j = \tfrac{1}{2} \dot{U}_m \, \text{diag} \, \phi_m(j) \, \phi_{im}^T \, m_i \, \phi_{in} \text{diag} \, \phi_n(j) \, \dot{U}_n = \text{Energy Transf. Funct.}$$

$$U_i{}^j = U_m \, \text{diag} \, \phi_m(j) \, \phi_{im}^T \, \phi_{in} \text{diag} \, \phi_n(j) \, U_n = \text{Displacement Transf. Funct.}$$

Table 4

Case	N	I	J	N*	I*	J*
1					12	2
2	960	480	480	13	24	2
3					12	4

Figure 8. COFS Space Truss Optimal Locations of Excitations and Sensors

GENERATING NEW SOLUTIONS

One of the key steps in the simulated annealing technique deals with how to create a new solution from the current one. In the examples discussed so far this was done by moving the J* excitations one at a time randomly to the remaining (J-J*) unassigned locations, and moving the I* sensors one at a time randomly to the remaining (I-I*) unassigned locations.

The following additional rules are now introduced to lend some insightful knowledge of the solution behavior into the otherwise highly randomized moves above.

1. RULES

a. Limit the excitation and sensor assignments to a smaller set of degree of freedom D* having relatively high modal displacements. $D* \supseteq D_1, D_2, ... D_{N*}$, where D_i set contains $\overline{N}$ degree-of-freedom ($\overline{N} \ll N$) with the largest displacement magnitudes in mode i. The size $\overline{N}$ is empirically chosen to be the largest of $\frac{1}{4} \sqrt{IxI*}$ and $\frac{1}{4} \sqrt{JxJ*}$.

b. From the expressions for $E_i{}^j$ one can show that $(E_i{}^j)_{i=j} \geq (E_i{}^j)_{i \neq j}$. Thus co-locating the J* excitations and I* sensors (whenever possible) will give the largest observable response. If $I* \neq J*$, the remaining ones are assigned independently.

c. As new solutions are generated, keep track of the best one so far. When θ is decremented, use this best solution as the starting point for the current temperature range.

Incorporation of the above rules in the policy for generating new solutions alter the simulated annealing implementation details - but not its basic philosophy. The changes are shown in Figure 9.
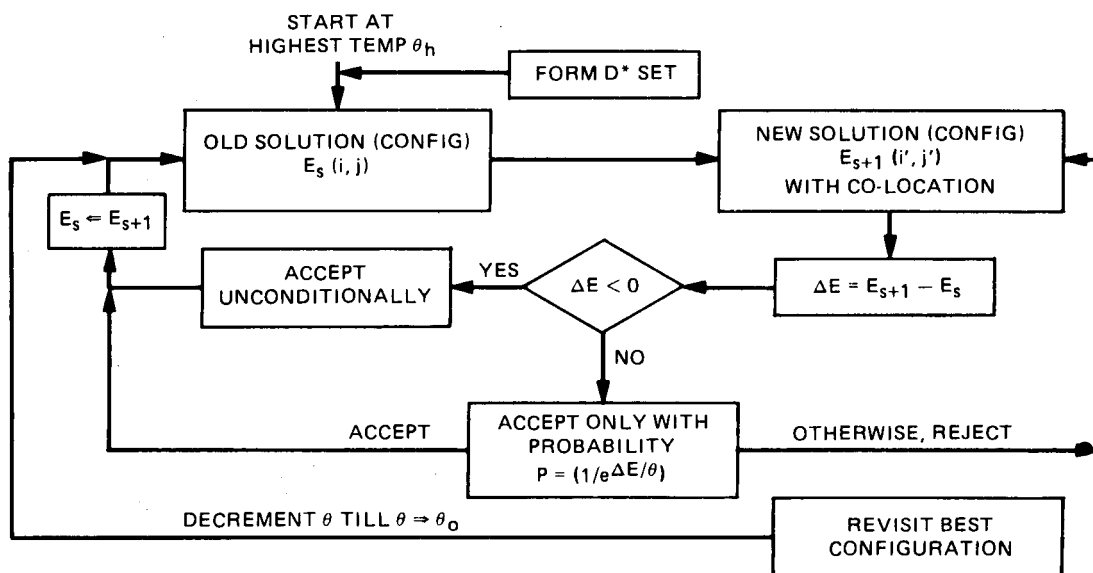

Figure 9.

2. NUMERICAL RESULTS

To assess the effect of the new solution generation rules of the previous section, the three cases of Table 4 were resolved with and without these rules. Table 5 compares the two sets of results using two measures: the maximum observed energy achieved at the end of the optimization schedule, and the CPU time required. The trend strongly supports the conclusion that the suggested rules help the simulated annealing algorithm in achieving more superior optima while requiring generally less computing time.

Figure 10 compares the set of actuator and sensor locations corresponding to the cases in Table 5.

Table 5

Max. Observed Energy for 13 Modes
(-:-) CPU Time

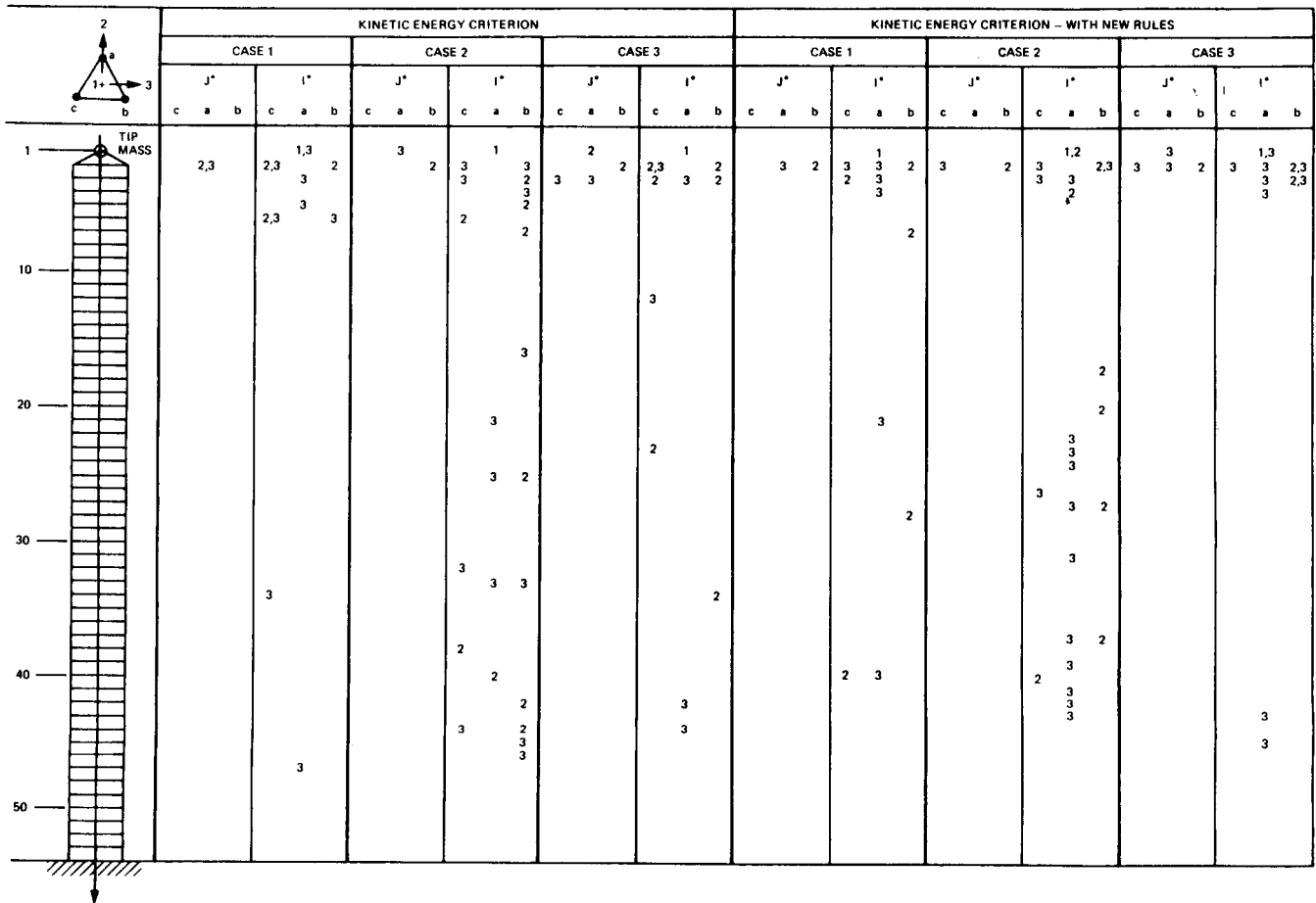|	Without New Rules	With New Rules
Case 1	5.37 (1:28)	6.61 (1:26)
Case 2	6.87 (2:18)	7.71 (2:24)
Case 3	9.62 (4:54)	9.72 (3:36)

Figure 10. COFS Space Truss Optimal Locations of Excitations and Sensors

CONCLUSIONS

The optimal placement of discrete actuators and sensors is posed as a combinatorial optimization problem. Two examples for truss structures were used for illustration; the first dealt with the optimal placement of passive dampers along existing truss members, and the second dealt with the optimal placement of a combination of a set of actuators and a set of sensors. Except for the simplest problems, an exact solution by enumeration involves a very large number of function evaluations, and is therefore computationally intractable. By contrast, the simulated annealing heuristic involves far fewer evaluations and is best suited for the class of problems considered. As an optimization tool, the effectiveness of the algorithm is enhanced by introducing a number of rules that incorporate knowledge about the physical behavior of the problem. Some of the suggested rules are necessarily problem dependent.

ACKNOWLEDGMENT

REFERENCES

1. Skelton, R. and DeLorenzo, M.,k "Selection of Noisy Actuators and Sensors in Linear Stochastic System," Journal of Large Scale Systems, Theory and Applications, pp. 109-136, 1983.

2. Haftka, R. and Adelman, H., "Damping and Control of Spacecraft Structures: Selection of Actuator Locations for Static Shape Control of Large Space Structures by Heuristic Integer Programming," Computers and Structures, Vol. 20, No. 1-3, pp. 575-582, 1985.

3. Salama, M., Rose, T., and Garba, J., "Optimal Placement of Excitations and Sensors for Verification of Large Dynamical Systems," 28th AIAA/ ASME/ASCE/AHS Structures, Structural Dynamics and Materials Conference, Paper No. 87-0782, Monterey, CA, April 1987.

4. Metropolis, N., Rosenbluth, A., Rosenbluth, M., Teller, A., and Teller, E., "Equations of State Calculations by Fast Computing Machines," Journal of Chemical Physics, Vol. 21, No. 6, pp. 1087-1092, June, 1953.